# Supporting information

**Synthesis and Hypergolic Properties of Flammable Ionic Liquids Based on the Cyano (1H-1,2,3-triazole-1-yl) dihydroborate Anion**

## Content

## 1. Single crystal data

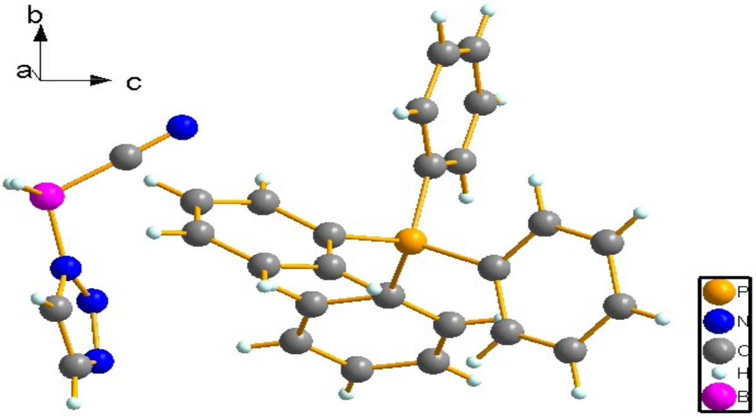

**Figure S1.** The single crystal of tetraphenylphosphonium cyano (1H-1,2,3-triazole-1-yl) dihydroborate

**Table S1**. Crystallographic data

| CCDC | 1853381 |
|---|---|
| Formula | $C_{27}H_{24}PBN_4$ |
| *Mr* | 446.28 |
| crystal system | Monoclinic |
| space group | P21/c |
| *a* [Å] | 8.170(2) |
| *b* [Å] | 14.187(4) |
| *c* [Å] | 20.986(6) |
| *α* [Å] | 90 |
| *β* [Å] | 92.499(8) |
| *γ* [Å] | 90 |
| *V* [Å$^3$] | 2430.1(11) |
| *Z* | 4 |
| *T* [K] | 173 |
| $\rho_{calcd}$ [Mg·m$^{-3}$] | 1.220 |
| M [mm$^{-1}$] | 0.135 |
| *F*(000) | 936.0 |
| *θ* [°] | 3.466 to 52.812 |
| index range | $-9 \leq h \leq 10$ |
|  | $-17 \leq k \leq 17$ |
|  | $-26 \leq l \leq 26$ |
| reflections collected | 18414 |
| independent reflections | 4922 [Rint = 0.0911, Rsigma = 0.0927] |

| | |
|---|---|
| data/restraints/paraneters | 4922/0/306 |
| GOF on $F^2$ | 1.002 |
| $R_1$ [I>2σ(I)] | 0.0540 |
| $wR_2$ [I>2σ(I)] | 0.1234 |
| $R_1$(all data) | 0.0951 |
| $wR_2$(all data) | 0.1450 |
| largest diff. peak and hole [e Å$^{-3}$] | 0.27/-0.36 |

## 2. Computational details

Theoretical calculations were performed by using the Gaussian 09 (Revision D.01) suite of programs.[1] For these new HILs, geometric optimization and frequency analyses were completed by using the B3LYP functional with the 6-31+G** basis set.[2] Single energy points were calculated at the MP2/6-311++G** level of theory. For all of the compounds, the optimized structures were characterized to be true local energy minima on the potential-energy surface without imaginary frequencies. Heats of formation (HOF, $\Delta_f H°$) of HILs were calculated based on a Born–Haber energy cycle (Fig. S2).

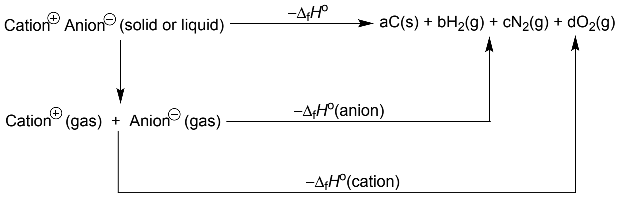

**Figure S2.** Born–Haber cycle for the formation of HILs; the number of moles of the respective products are given by a, b, c, and d.

For all the HILs, calculation of the HOFs was simplified by using Equation (1),[3] in which $\Delta_L H°$ was the lattice energy of the salts.

$$\Delta_f H° \text{ (HILs, 298K)} = \Sigma\Delta_f H°\text{(cation, 298K)} + \Sigma\Delta_f H°\text{(anion, 298K)} - \Delta_L H° \qquad (1)$$

For 1:1 salts, and considering the nonlinear nature of the cations and anion used, $\Delta_L H°$ (kJ mol$^{-1}$) was predicted by using Equation (2), as suggested by Jenkins et al.,[4] in which $n_M$ and $n_X$ depended on the nature of ions $M_p^+$ and $X_q^-$, respectively, and had a value of 6 for nonlinear polyatomic ions.

$$\Delta_L H° = U_{POT} + [p(n_M/2-2) + q(n_X/2-2)]RT \qquad (2)$$

The lattice-potential energy ($U_{POT}$) was calculated according to Equation (3),[5] in which $\rho_m$ is the density (g cm$^{-3}$) and $M_m$ is the chemical formula mass of the ionic material.

$$U_{POT}\ (\text{kJ mol}^{-1}) = 1981.2(\rho_m/M_m)^{1/3} + 103.8 \quad (3)$$

$$\Delta_f H_{(g)C}{}^{+\circ} = \Delta_f H_{(g)C}{}^{\circ} + IE_C \quad (4)$$

$$\Delta_f H_{(g)A}{}^{-\circ} = \Delta_f H_{(g)A}{}^{\circ} + EA_A \quad (5)$$

The heats of formation (HOFs) of the ionic salts were obtained by computing the component cations and anions. Specifically, the computation of HOFs for both the cations and anions was performed according to literature methods,[6] that is, the gas-phase HOFs of the ions were determined by using Equations (4) and (5) (*IE* = ionization energy; *EA* = electron affinity). In Equations (4) and (5), additional calculations for the corresponding neutral molecules ($\Delta H_{f(g)C}{}^{\circ}$ and $\Delta H_{f(g)A}{}^{\circ}$) were performed for the atomization reaction $C_aH_bN_cO_dP_eB_f \rightarrow aC(g) + bH(g) + cN(g) + dO(g) + eP(g) + fB(g)$ by using G2 theory. Based on the results from Equation (4), the HOFs of the cations were obtained by using isodesmic reactions (Figure S3. ).

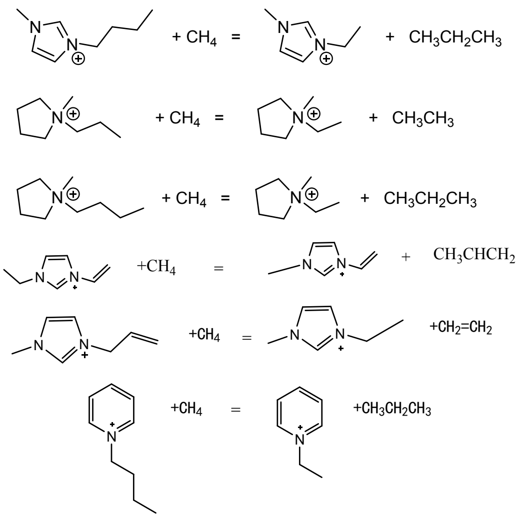

**Figure S3.** Isodesmic reactions for the HOFs calculation.

The enthalpy of reaction ($\Delta_r H^{\circ}_{298}$) was obtained by combining the MP2/6-311++G** energy difference for the reaction, the scaled zero-point energies, and other thermal factors. As a result, the heats of formation of all HILs could be readily extracted. By using the calculated heats of formation and the experimentally measured densities, the specific impulses of these new HILs were calculated by using Explo5 (v6.02).

The computational details of heats of formation ($\Delta_f H$) and specific impulse ($I_{sp}$) are listed as follow:

**Table S2.** Enthalpies of the gas-phase speciesofcations and anions (based on G2 method)

| ions | $\Delta H_f$（kJ·mol$^{-1}$） |
|---|---|
| 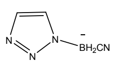 | 52.38 |
| 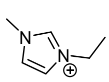 | 640.1 |
| 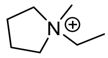 | 502.0 |
| 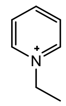 | 292.3 |

**Table S3.** Enthalpies of the gas-phase species of anions and cations based on isodesmic reactions

| ions | E(MP2)$^a$ | ZPE$^b$ | TCH$^c$ | $\Delta H_{corr}$ | $\Delta H_f$（kJ·mol$^{-1}$） |
|---|---|---|---|---|---|
| 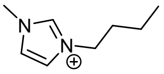 | -422.0 | 0.2259 | 0.2380 | -40.33 | 596.9 |
| 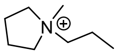 | -369.1 | 0.2577 | 0.2689 | -40.33 | 479.4 |
| 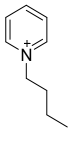 | -404.8 | 0.2155 | 0.2265 | -40.33 | 647.0 |
| 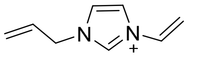 | -419.55 | 0.1786 | 0.1894 | -40.33 | 858.9 |
| 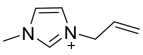 | -381.58 | 0.1840 | 0.1669 | -40.33 | 750.0 |

**Table S4.** Thecalculated HOFs of HILs

| HILs | $\Delta H_{cation}$ (kJ·mol$^{-1}$) | $\Delta H_{anion}$ (kJ·mol$^{-1}$) | $\Delta H_{lat}$ (kJ·mol$^{-1}$) | $\Delta H_{f}$ （kJ·mol$^{-1}$） |
|---|---|---|---|---|
| IL-1 | 750.0 | 52.4 | 443.7 | 358.7 |
| IL-2 | 859.0 | 52.4 | 439.7 | 471.6 |
| IL-3 | 640.1 | 52.4 | 450.1 | 242.3 |
| IL-4 | 596.9 | 52.4 | 433.0 | 216.2 |
| IL-5 | 502.03 | 52.4 | 442.7 | 111.7 |
| IL-6 | 479.4 | 52.4 | 434.7 | 97.0 |
| IL-7 | 458.2 | 52.4 | 427.3 | 83.2 |
| IL-8 | 691.9 | 52.4 | 452.0 | 292.3 |
| IL-9 | 646.7 | 52.4 | 433.6 | 265.8 |

## 3. Ignition test with $H_2O_2$

In this work, we added 15 wt% iodine into HL-1-3 and used 90% $H_2O_2$ as an oxidizer in the droplet test. IL-1-3 can be ignited after adding iodine. It seems that iodine could effectively promote hypergolic reactions between these boron-containing ILs and $H_2O_2$ (90 %) oxidizer. The ID times of these three ILs were IL-1 (2 s), IL-2 (3 s), and IL-3 (2.7 s), respectively. Additional studies will be conducted in the future.

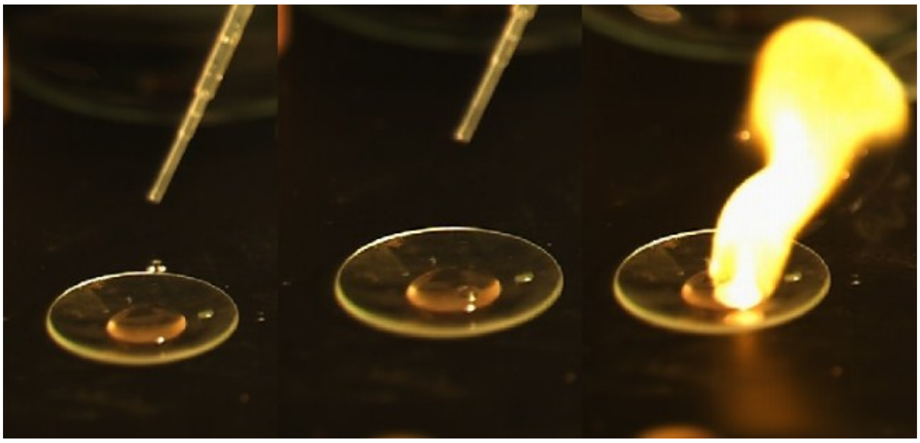

**Figure S4.** Droplet tests carried out on IL-1 with 90% $H_2O_2$

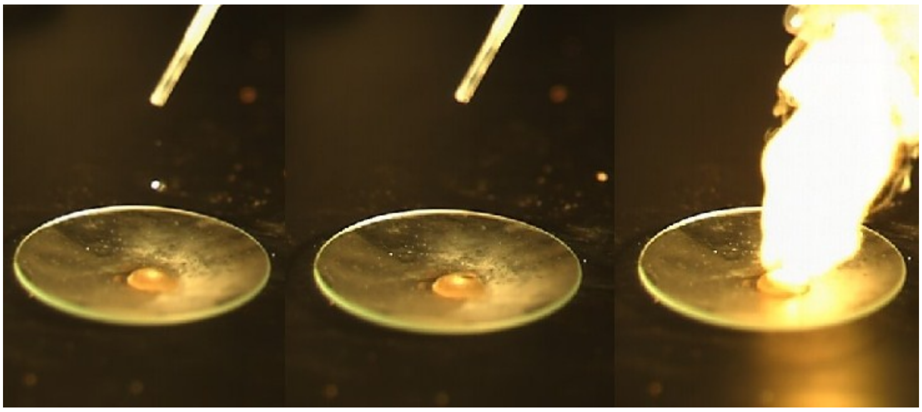

**Figure S5.** Droplet tests carried out on IL-2 with 90% $H_2O_2$

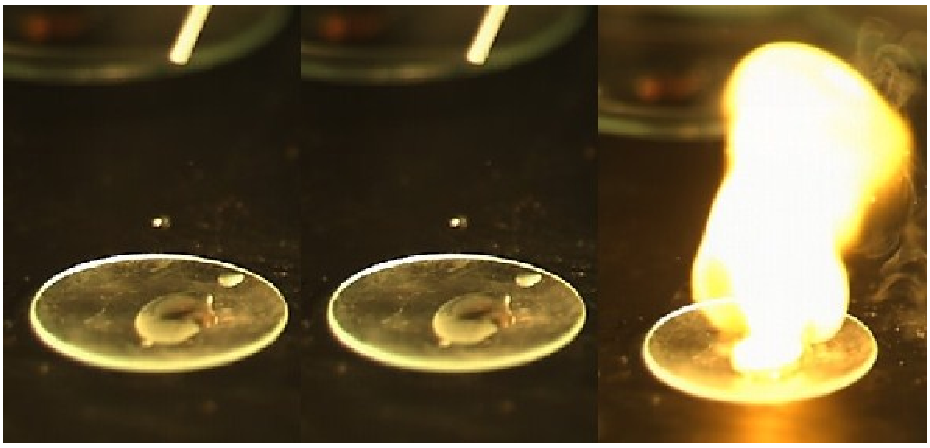

**Figure S6.** Droplet tests carried out on IL-3 with 90% $H_2O_2$

## 4. Spectra of NMR

**All of the product using deuterated acetonitrile as test solvent**

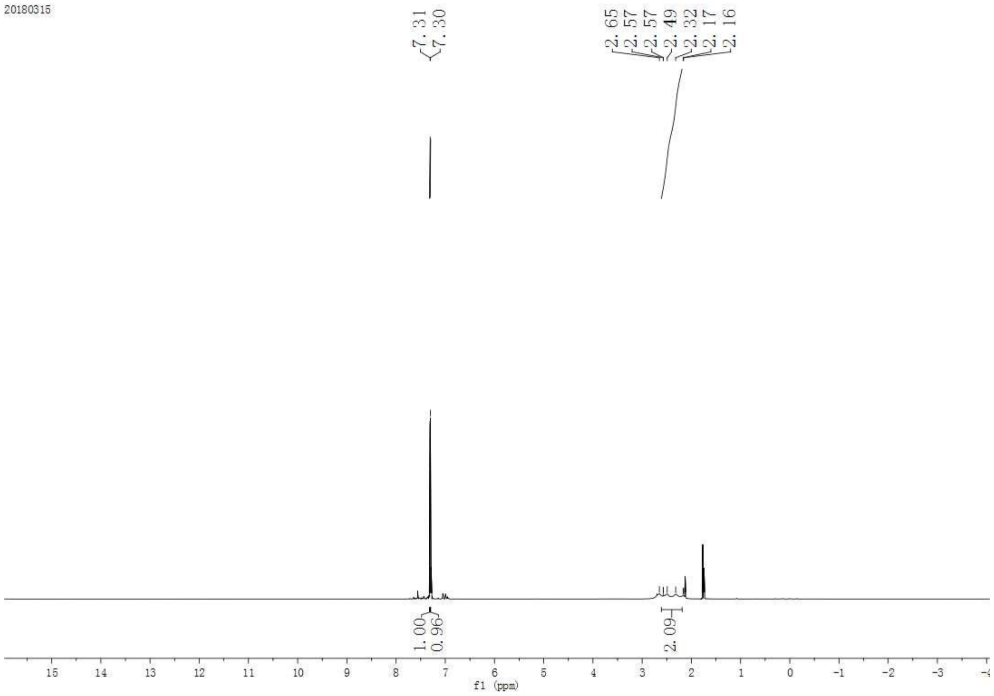

Figure S7. $^{1}H$-NMR of sodium cyano(1H-1,2,3-triazole-1-yl)dihydroborate (1)

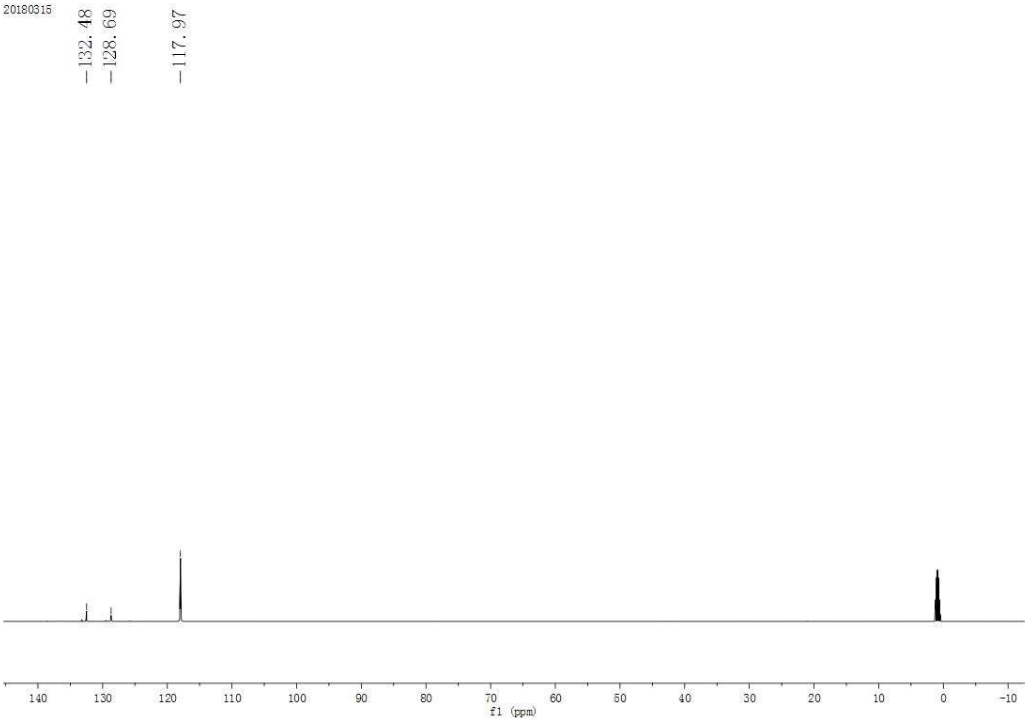

Figure S8. $^{13}C$-NMR of sodium cyano(1H-1,2,3-triazole-1-yl)dihydroborate (1)

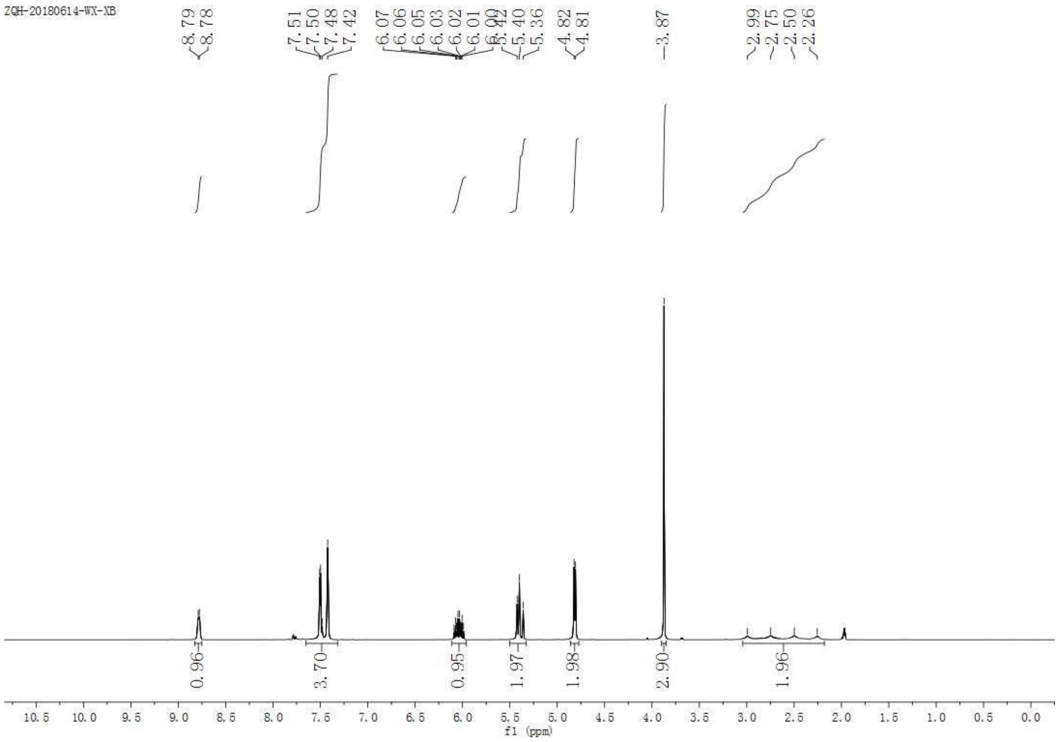

**Figure S9.** $^{1}$H-NMR of 1-methyl-3-allylimidazolium cyano (1H-1,2,3-triazole-1-yl) dihydroborate (IL-1)

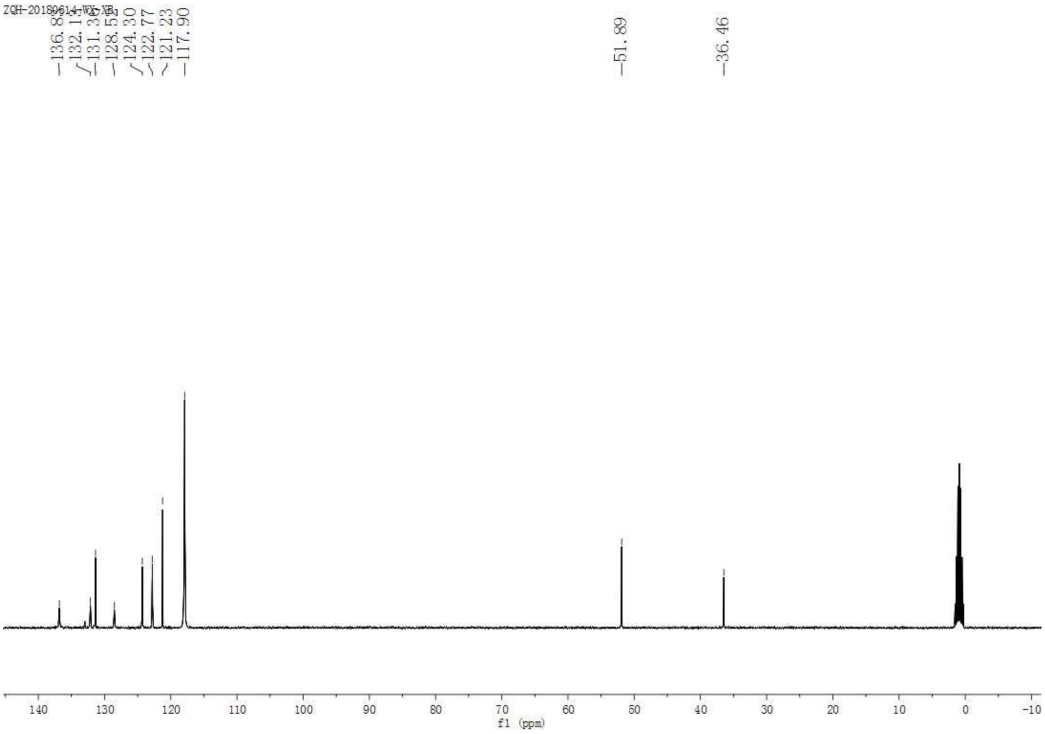

**Figure S10.** $^{13}$C-NMR of 1-methyl-3-allylimidazolium cyano (1H-1,2,3-triazole-1-yl) dihydroborate (IL-1)

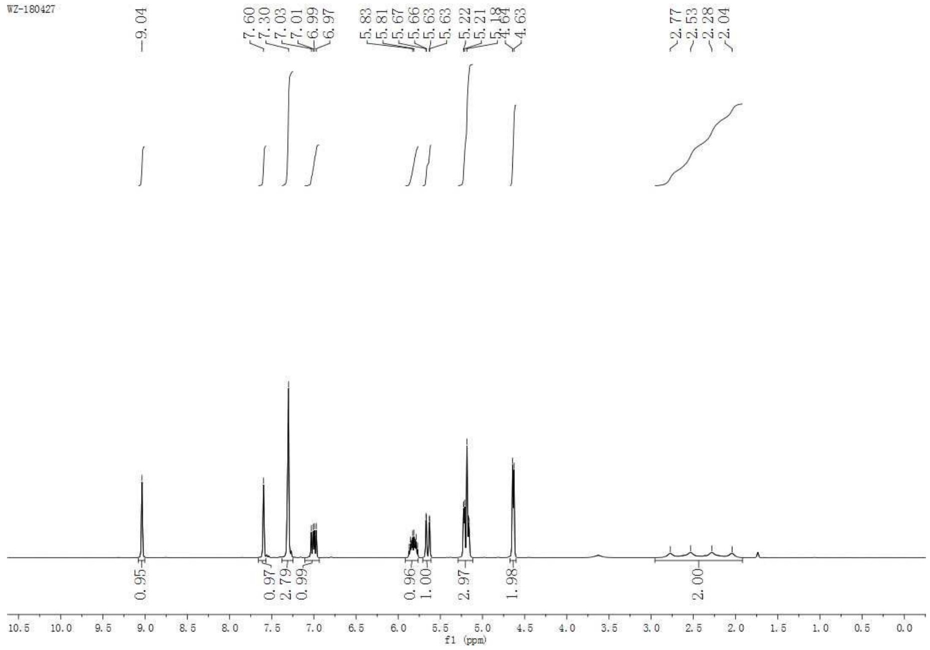

Figure S11. $^{1}H$-NMR of 1-allyl-3-vinylimidazolium cyano (1H-1,2,3-triazole-1-yl) dihydroborate (IL-2)

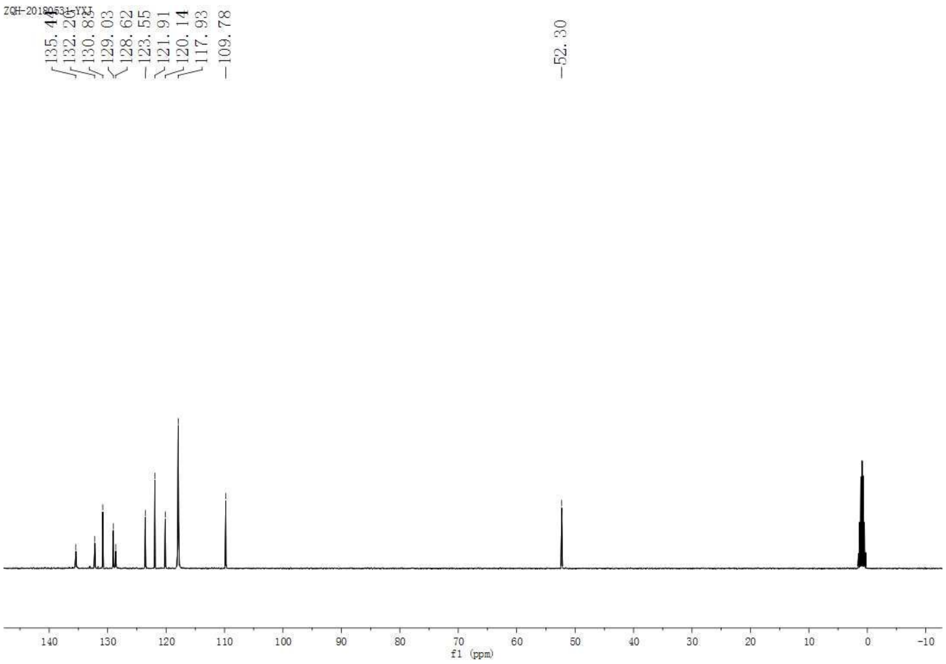

Figure S12. $^{13}C$-NMR of 1-allyl-3-vinylimidazolium cyano (1H-1,2,3-triazole-1-yl) dihydroborate (IL-2)

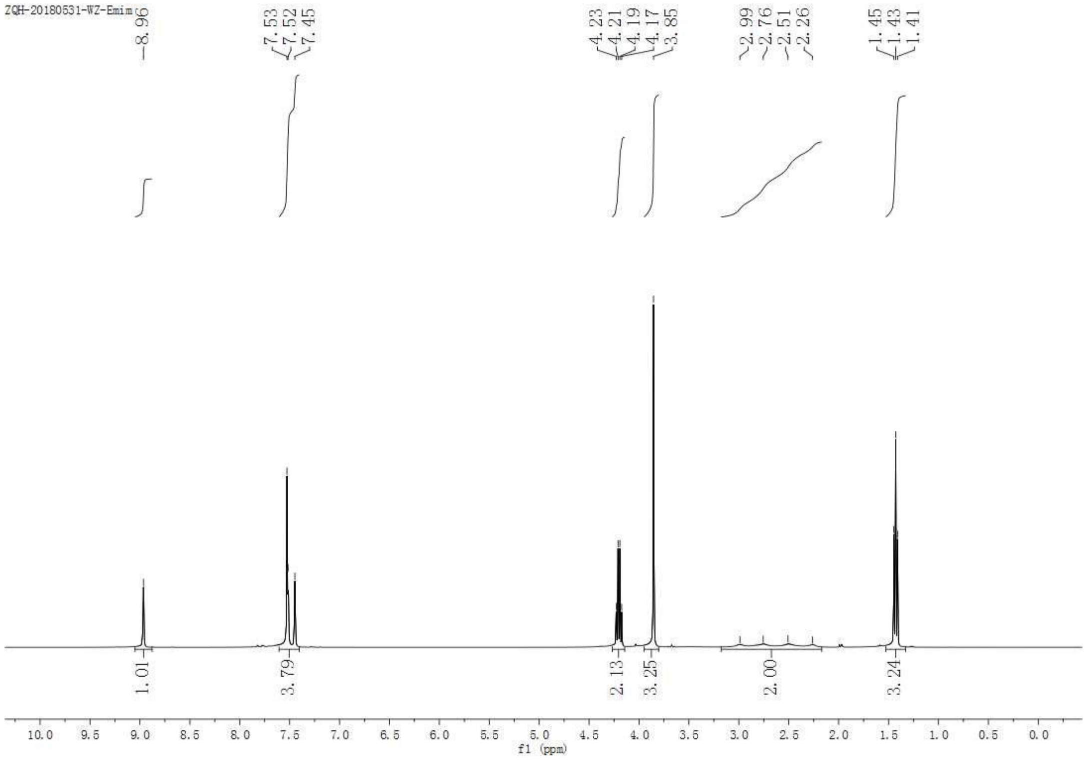

**Figure S13.** $^1$H-NMR of 1-ethyl-3-methylimidazolium cyano (1H-1,2,3-triazole-1-yl) dihydroborate (IL-3)

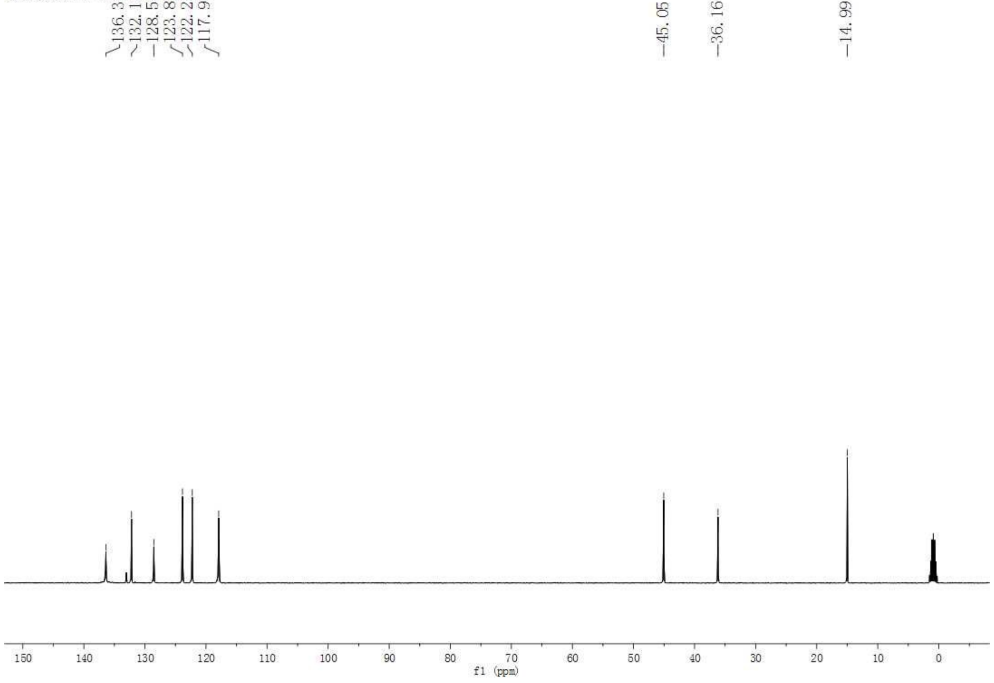

**Figure S14.** $^{13}$C-NMR of 1-ethyl-3-methylimidazolium cyano (1H-1,2,3-triazole-1-yl) dihydroborate (IL-3)

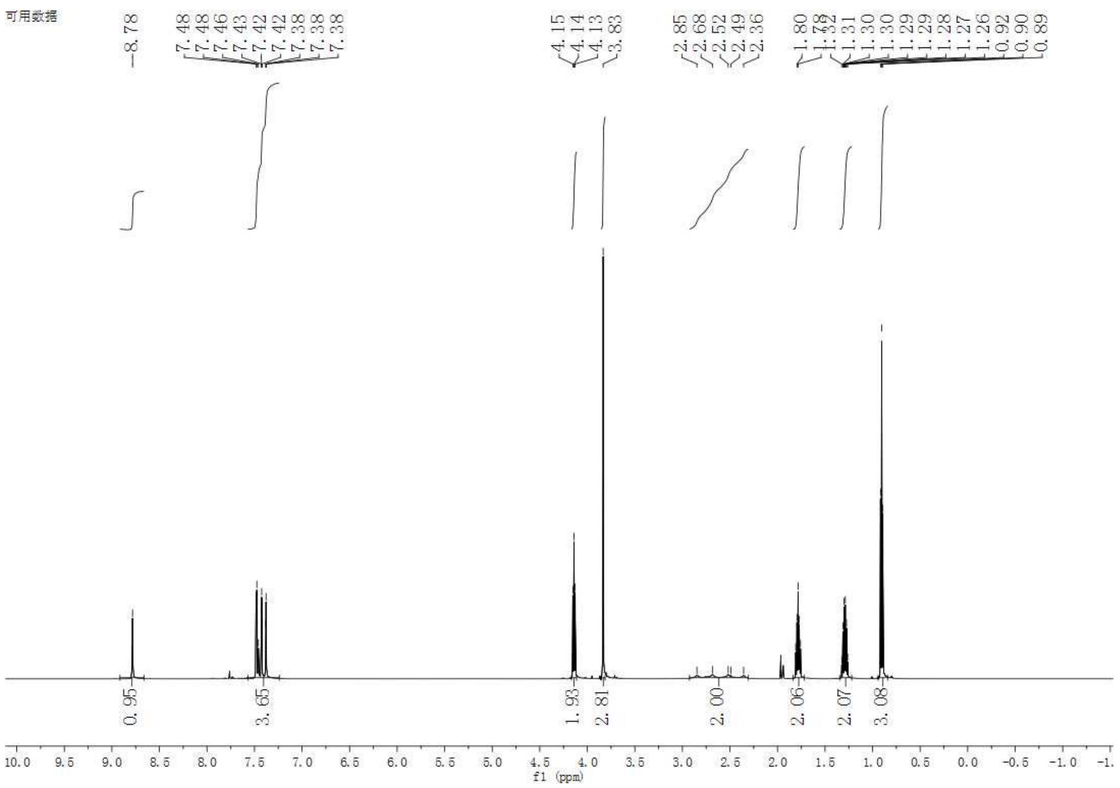

Figure S15. $^1$H-NMR of 1-butyl-3-methylimidazolium cyano (1H-1,2,3-triazole-1-yl) dihydroborate (IL-4)

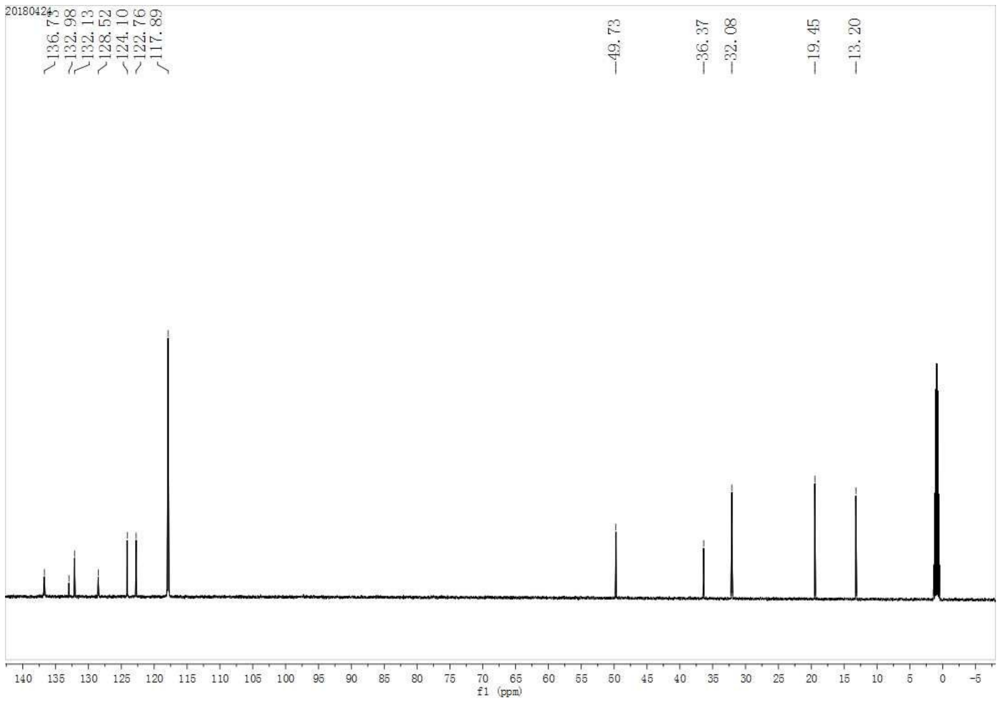

Figure S16. $^{13}$C-NMR of 1-butyl-3-methylimidazolium cyano (1H-1,2,3-triazole-1-yl) dihydroborate (IL-4)

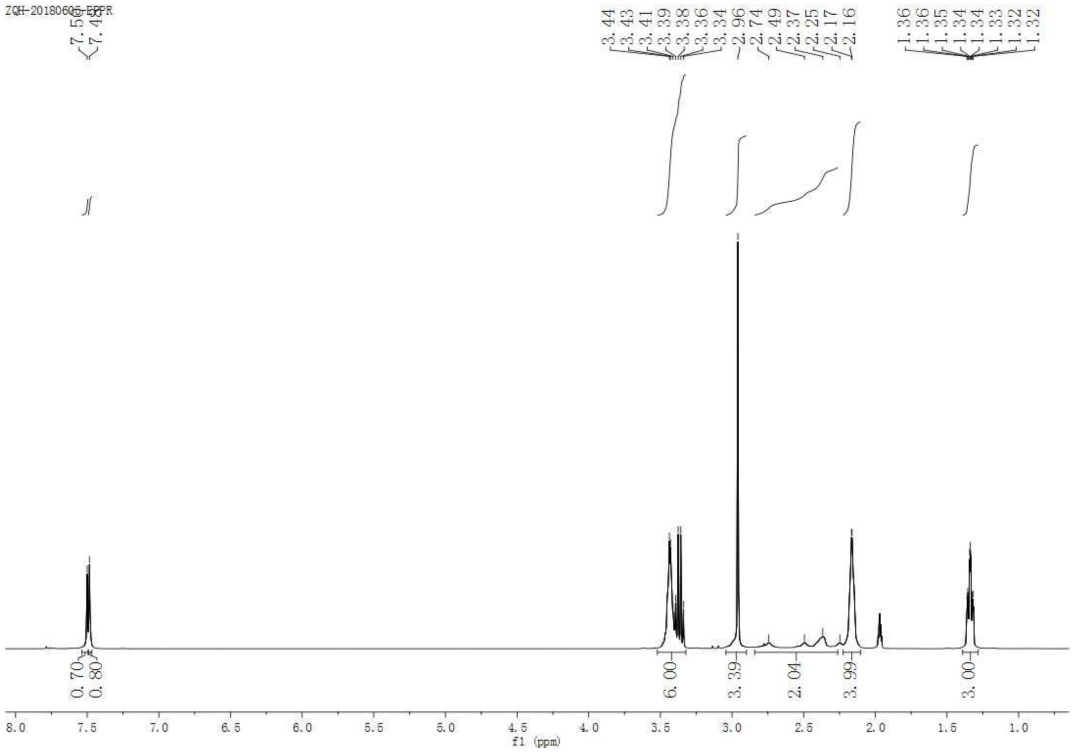

**Figure S17.** $^1$H-NMR of 1-ethyl-1-methylpyrrolidin cyano (1H-1,2,3-triazole-1-yl) dihydroborate (IL-5)

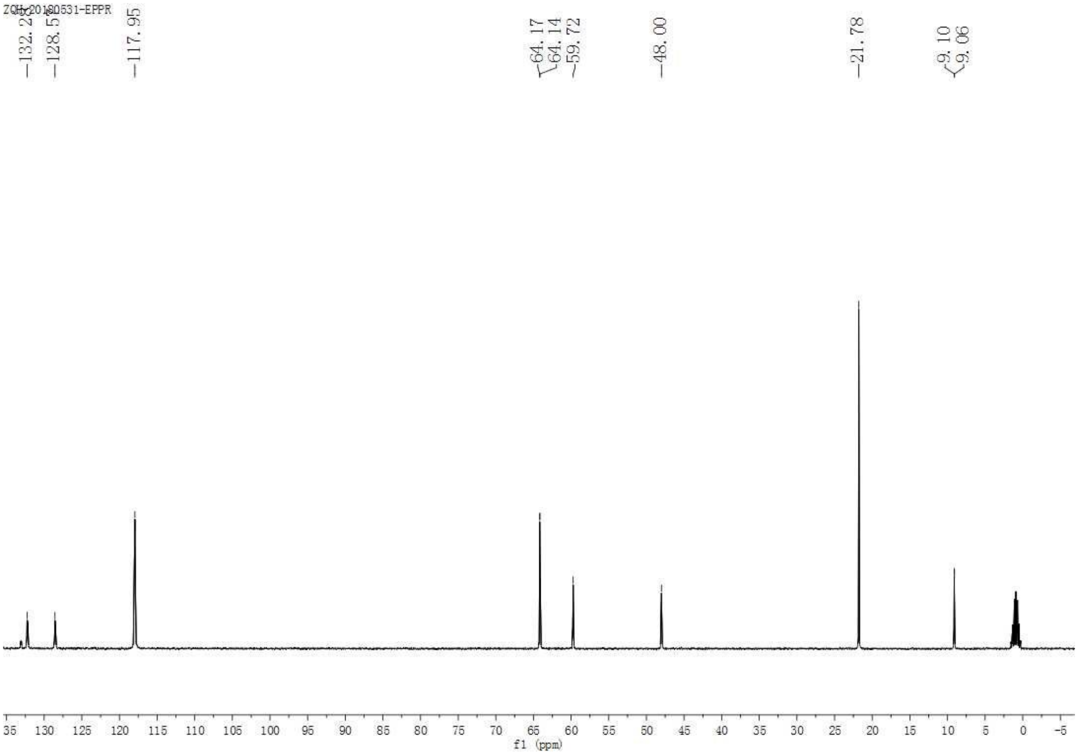

**Figure S18.** $^{13}$C-NMR of 1-ethyl-1-methylpyrrolidin cyano (1H-1,2,3-triazole-1-yl) dihydroborate (IL-5)

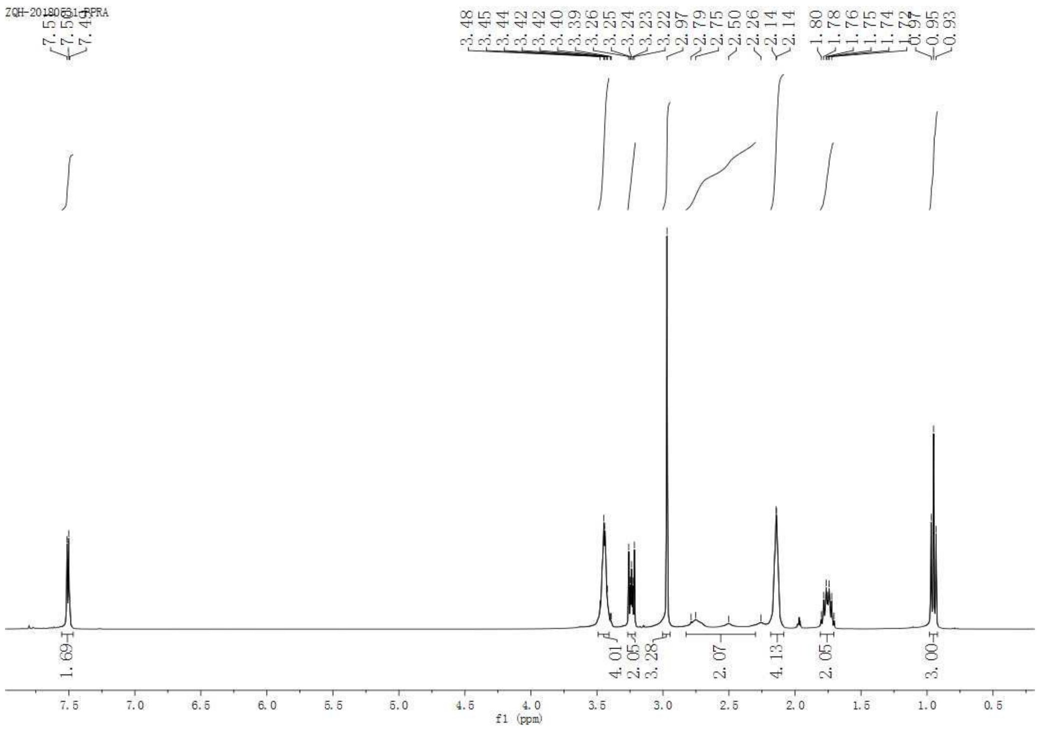

**Figure S19.** $^1$H-NMR of 1-propyl-1-methylpyrrolidin cyano (1H-1,2,3-triazole-1-yl) dihydroborate (IL-6)

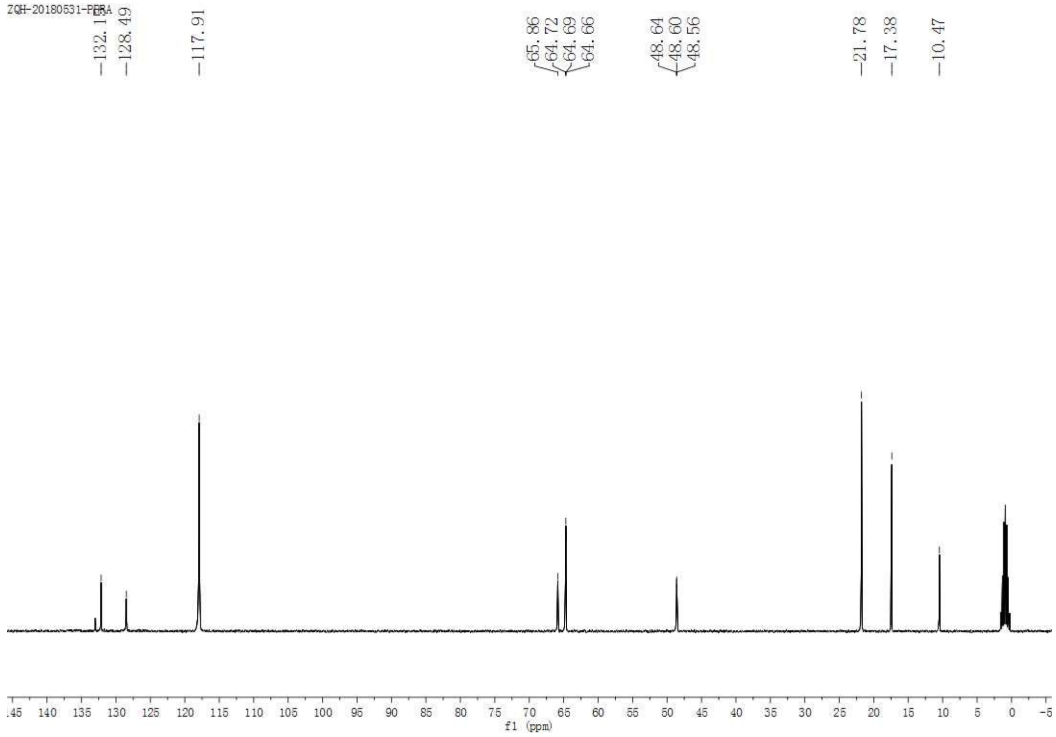

**Figure S20.** $^{13}$C-NMR of 1-propyl-1-methylpyrrolidin cyano (1H-1,2,3-triazole-1-yl) dihydroborate (IL-6)

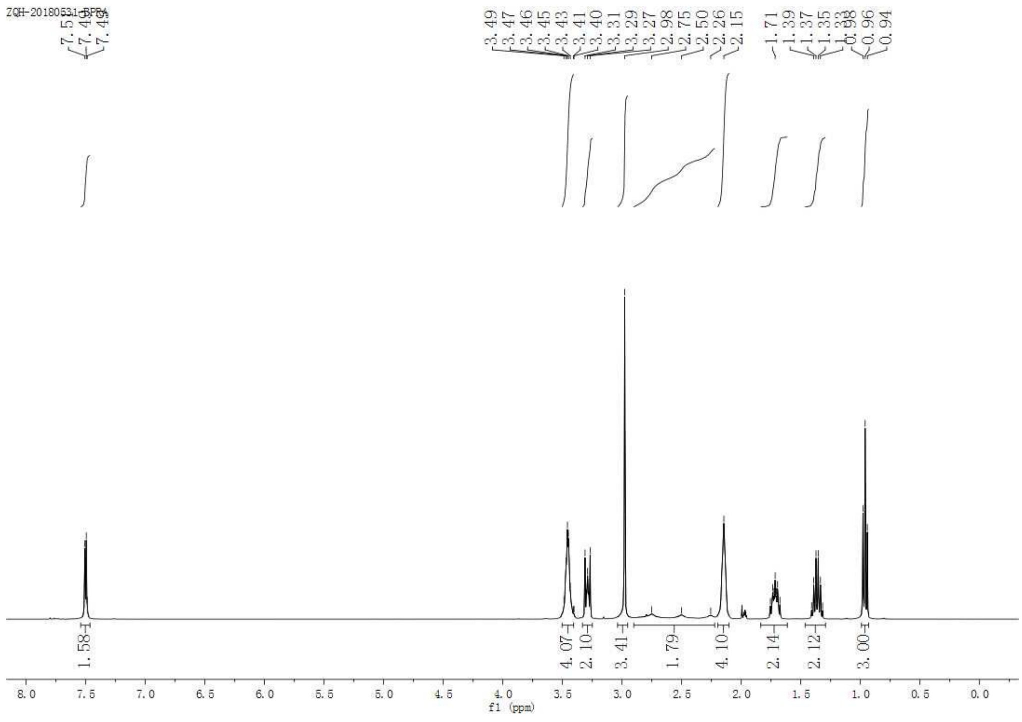

**Figure S21.** $^1$H-NMR of 1-butyl-1-methylpyrrolidin cyano (1H-1,2,3-triazole-1-yl) dihydroborate (IL-7)

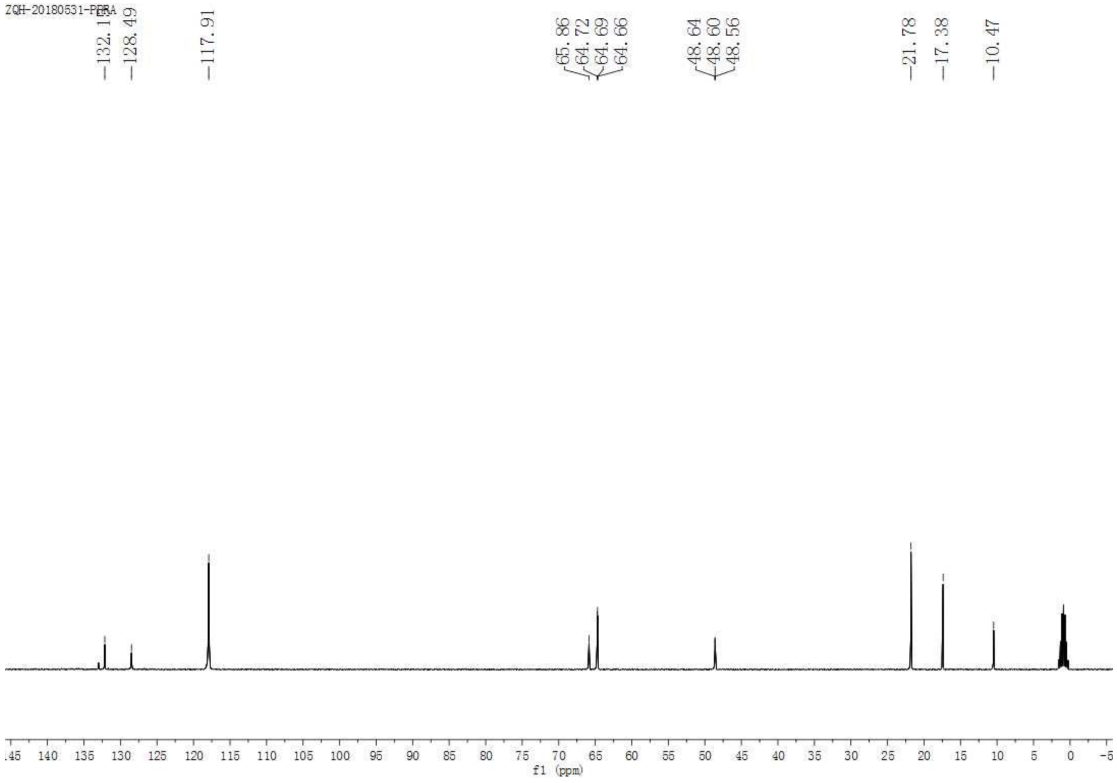

**Figure S22.** $^{13}$C-NMR of 1-butyl-1-methylpyrrolidin cyano (1H-1,2,3-triazole-1-yl) dihydroborate (IL-7)

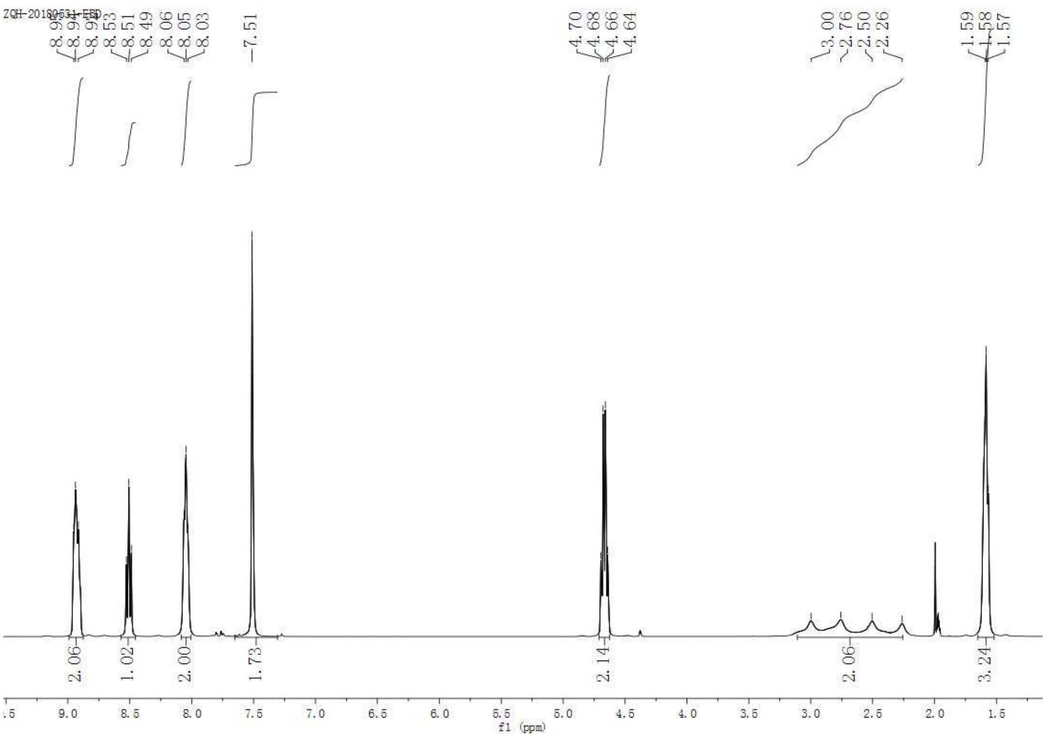

**Figure S23.** $^{1}$H-NMR of N-ethylpyridine cyano(1H-1,2,3-triazole-1-yl)dihydroborate (IL-8)

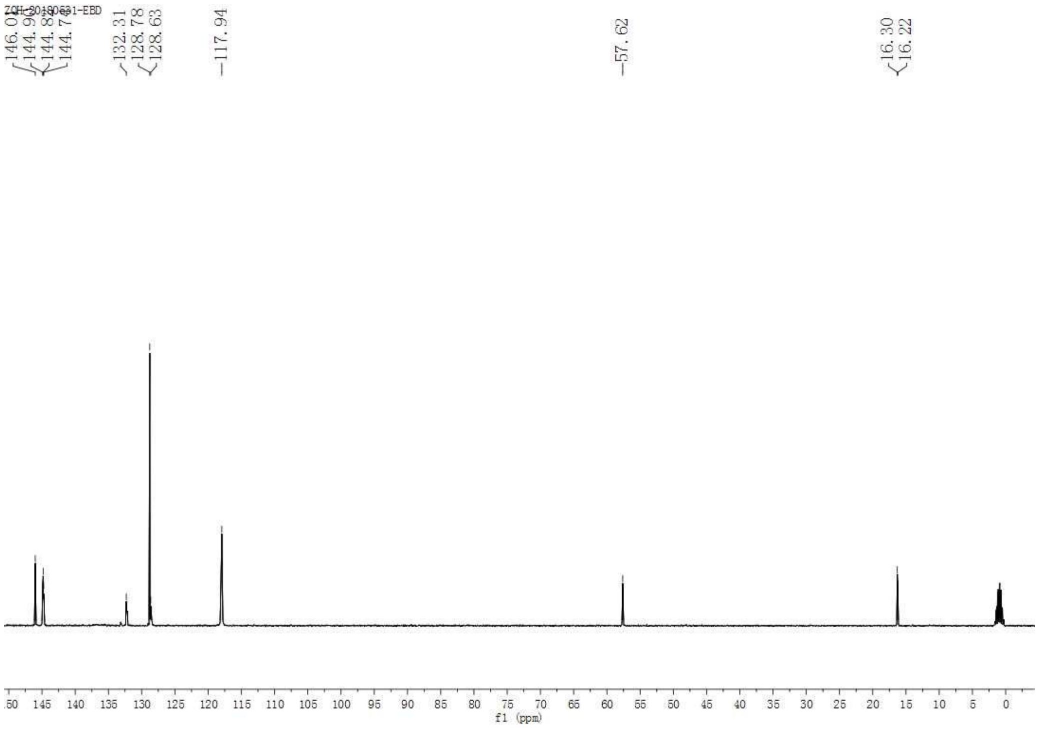

**Figure S24.** $^{13}$C-NMR of N-ethylpyridine cyano(1H-1,2,3-triazole-1-yl)dihydroborate (IL-8)

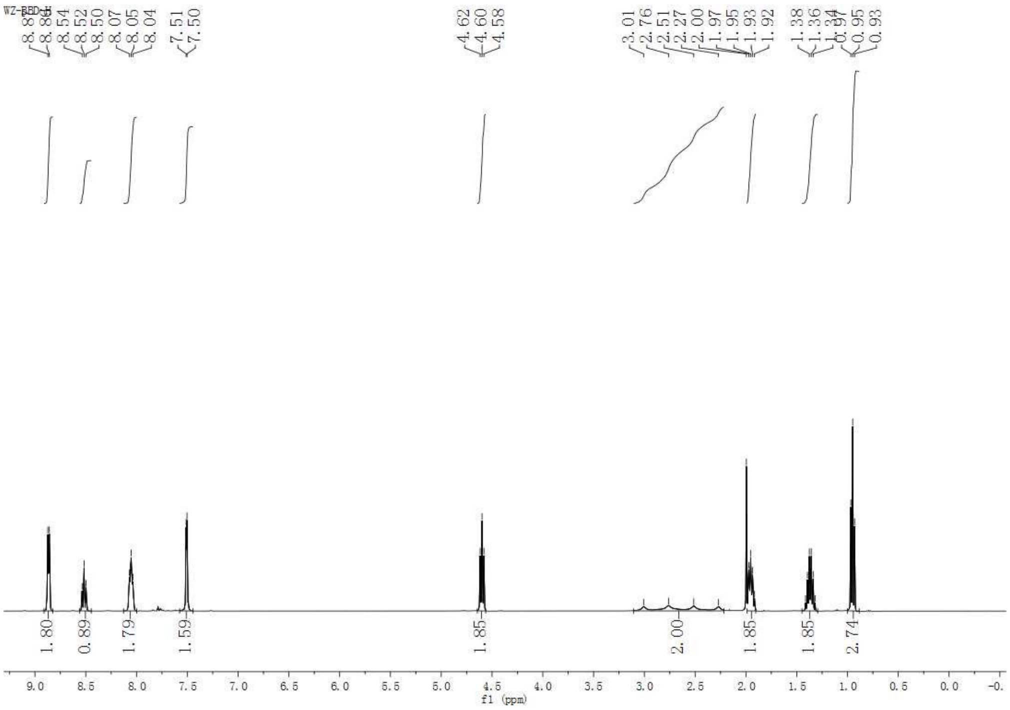

Figure S25. $^{1}$H-NMR of N-butylpyridine cyano(1H-1,2,3-triazole-1-yl)dihydroborate (IL-9)

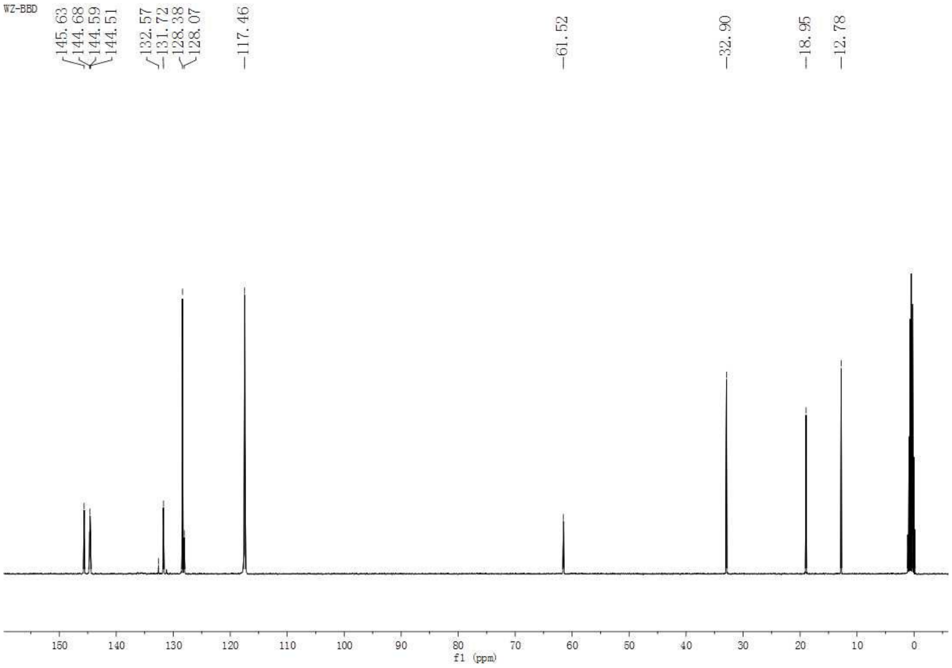

Figure S26. $^{13}$C-NMR of N-butylpyridine cyano(1H-1,2,3-triazole-1-yl)dihydroborate (IL-9)

## Reference

[1] Gaussian 09, Revision D. 01, M. J. Frisch et al., Gaussian Inc., Wallingford CT, 2009.

[2] R. G. Parr, W. Yang, *Density Functional Theory of Atoms and Molecules,* Oxford University Press, New York, 1989.

[3] L. A. Curtiss, K. Raghavachari, G. W. Trucks, J. A. Pople, *J. Chem. Phys.*, 1991, **94**, 7221.

[4] H. D. B. Jenkins, D. Tudela, L. Glasser, *Inorg. Chem.*, 2002, **41**, 2364.

[5] S. Bastea, L. E. Fried, K. R. Glaesemann, W. M. Howard, P. C. Souers, P. A.Vitello, *Cheetah 5.0 User's Manual*, Lawrence Livermore National Laboratory, Livermore, 2007.

[6] (a) H. D. B. Jenkins, H. K. Roobottom, J. Passmore, L. Glasser, *Inorg. Chem.*, 1999, **38**, 3609; (b) B. M. Rice, E. F. C. Byrd, W. D. Mattson. Computational Aspects of Nitrogen-Rich HEDMs, Chapter 5, in *High Energy Density Materials (Structure and Bonding)*. T. M. Klapötke*,* Ed., Springer, Berlin, 2007, pp. 153.